

Contents lists available at ScienceDirect

Physics Letters B

www.elsevier.com/locate/physletb

Electromagnetic properties of dark matter: Dipole moments and charge form factor

Vernon Barger^a, Wai-Yee Keung^b, Danny Marfatia^{c,*}^a Department of Physics, University of Wisconsin, Madison, WI 53706, USA^b Department of Physics, University of Illinois, Chicago, IL 60607, USA^c Department of Physics and Astronomy, University of Kansas, Lawrence, KS 66045, USA

ARTICLE INFO

Article history:

Received 3 September 2010

Received in revised form 1 December 2010

Accepted 2 December 2010

Available online 8 December 2010

Editor: S. Dodelson

Keywords:

Dark matter

Electric dipole moment

Magnetic dipole moment

Electric charge form factor

ABSTRACT

A neutral dark matter particle may possess an electric dipole moment (EDM) or a magnetic dipole moment (MDM), so that its scattering with nuclei is governed by electromagnetic interactions. If the moments are associated with relevant operators of dimension-5, they may be detectable in direct search experiments. We calculate complete expressions of the scattering cross sections and the recoil energy spectra for dark matter with these attributes. We also provide useful formulae pertinent to dark matter that interacts via an electric charge form factor (CFF) which is related to the charge radius defined by an effective dimension-6 operator. We show that a 7 GeV dark matter particle with an EDM, MDM or CFF easily reproduces the CoGeNT excess while remaining consistent with null searches.

© 2010 Elsevier B.V. Open access under [CC BY license](http://creativecommons.org/licenses/by/3.0/).

1. Introduction

The nature of the dark matter (DM) particle is unknown. There are many well studied scenarios guided by theoretical niceties such as the Minimal Supersymmetric Standard Model, models with extra dimensions, and the Little Higgs Models with T -parity, all of which posit that the DM particle interacts primarily via weak interactions. On the experimental side, direct DM searches are looking for signals of the recoiling nuclei from DM–nucleus scattering. We take the uncommon view that the scattering process may be electromagnetic in nature. The interaction occurs through the electric dipole moment (EDM) or the magnetic dipole moment (MDM) of dark matter. The interactions are described by dimension-5 operators for non-self-conjugate particles, such as Dirac DM, but not for Majorana DM. The EDM and MDM of DM can be induced by underlying short distance physics at the one-loop order or higher. As there are no strong reasons against large CP violation in the DM sector, we cannot neglect the EDM possibility. In fact, for comparable short distance cutoffs, we find that an EDM may give the dominant contribution to DM–nucleus scattering because it directly couples to the nuclear charge. In the EDM case, the recoil energy E_R distribution is highly enhanced in the low E_R region as $1/(v_r^2 E_R)$ (where v_r is the speed of the DM particle in the rest

frame of the nucleus) in contrast with that from MDM which goes as $1/E_R$.

While DM–nucleus scattering due to the MDM of DM has been studied extensively in the literature, the relevant formulae with the correct dependence on the nuclear charge Z and nuclear moment $\mu_{Z,A}$ are not available. In this work, we provide analytic expressions for the scattering cross sections for the MDM and EDM cases with careful expansions in the relative velocity and recoil energy. To complete the treatment of electromagnetic properties of DM, we extend our analysis to the dimension-6 operator, which is the electric charge form factor (CFF) slope or the charge radius of the neutral DM. The operator has a structure that is similar to that of the spin-independent (SI) interaction.

2. Electric dipole moment of dark matter

The effective non-relativistic Hamiltonian of the EDM of a particle with spin \mathbf{S} is

$$H_{\text{eff}} = -\mathfrak{d} \mathbf{E} \cdot \mathbf{S}/S,$$

with the normalization chosen to agree with the standard form for a spin $\frac{1}{2}$ particle, i.e., $-\mathfrak{d} \mathbf{E} \cdot \boldsymbol{\sigma}$, where \mathfrak{d} is dimensionful, and the electromagnetic energy density is $(E^2 + B^2)/2$. As the electric field of the nucleus $\mathbf{E} = -\text{grad} \phi$, we identify the gradient with the momentum transfer \mathbf{q} . Therefore, the direct scattering of the DM particle χ and the nucleus N , $\chi N \rightarrow \chi N$, via the interaction

* Corresponding author.

E-mail address: marfatia@ku.edu (D. Marfatia).

between the DM electric dipole (with moment d_χ) and the nuclear charge Ze (with $e^2 = 4\pi\alpha$) is

$$\mathcal{M} = \mathbf{S} \cdot i\mathbf{q} \left(\frac{d_\chi}{S} \frac{1}{q^2} Ze \right).$$

It is important to note that the momentum transfer \mathbf{q} is Galilean invariant and is conveniently related to the center-of-mass momentum \mathbf{p} . Hence $d\mathbf{q}^2 = 2|\mathbf{p}|^2 d\cos\theta = 4|\mathbf{p}|^2 \frac{d\Omega}{4\pi}$, and $|\mathbf{p}| = m_r v_r$, where $m_r \equiv \frac{m_A m_\chi}{m_A + m_\chi}$ is the reduced mass; m_A and m_χ are the masses of the nucleus and DM particle, respectively. q^2 ranges from 0 to $(2m_r v_r)^2$, as is easily checked in the center-of-mass frame in which the momenta have equal magnitudes $m_r v_r$.¹ We use the spin relation,

$$\text{Tr}(S^i S^j) = (2S + 1)\delta^{ij} S(S + 1)/3,$$

to obtain the spin-averaged differential cross section,

$$d\sigma_{EDM}(\chi N) = \frac{1}{4\pi} d_\chi^2 Z^2 e^2 \frac{(S + 1)}{3S} \frac{1}{v_r^2} \frac{d\mathbf{q}^2}{q^2} |G_E(\mathbf{q}^2)|^2. \quad (1)$$

We have included the nuclear charge form factor $|G_E(\mathbf{q}^2)|^2$ to incorporate elastic scattering effects off a heavy nucleus.² Accounting for a difference in convention in the definition of e , our formula agrees with that of Ref. [6].

We relate q^2 to the nuclear recoil energy in the lab frame, $q^2 = 2m_A E_R$, and find

¹ The DM particle velocity in the frame of the galactic halo is usually described [1] by a Maxwellian distribution,

$$f^G(\mathbf{v}) d^3\mathbf{v} = \frac{N}{(v_0 \sqrt{\pi})^3} e^{-v^2/v_0^2} d^3\mathbf{v},$$

where the most probable velocity is $v_0 = 230$ km/s, and the distribution is cut off at the escape velocity $v_{\text{esc}} = 600$ km/s. The normalization N is close to 1, or more precisely,

$$N = \frac{1}{\text{erf}(v_{\text{esc}}/v_0) - \frac{2}{\sqrt{\pi}}(v_{\text{esc}}/v_0) \exp(-v_{\text{esc}}^2/v_0^2)}.$$

The one-variable velocity distribution is

$$f_1^G(v) dv = \frac{4v^2 N}{v_0^3 \sqrt{\pi}} e^{-v^2/v_0^2} dv.$$

However, since the solar system is moving at a speed $v_E = 244$ km/s with respect to the halo [2] and $v_E \sim v_0$, we need to use a more relevant distribution of the relative velocity, $\mathbf{v}_r = \mathbf{v} - \mathbf{v}_E$. As an approximation we ignore the seasonal motion of the Earth around the Sun with a relative speed of about 30 km/s. Then,

$$f(\mathbf{v}_r) d^3\mathbf{v}_r = f^G(\mathbf{v}) d^3\mathbf{v} = f^G(\mathbf{v}_r + \mathbf{v}_E) d^3\mathbf{v}_r \quad \text{because } d^3\mathbf{v} = d^3\mathbf{v}_r.$$

For a fixed v_r , we integrate the polar angle between \mathbf{v}_r and \mathbf{v}_E to obtain

$$f_1(v_r) dv_r = N \frac{v_r dv_r}{v_E v_0 \sqrt{\pi}} \left(e^{-(\min(v_r - v_E, v_{\text{esc}}))^2/v_0^2} - e^{-(\min(v_r + v_E, v_{\text{esc}}))^2/v_0^2} \right).$$

If $v_r > v_{\text{esc}} + v_E$, $f_1(v_r) = 0$; see Refs. [1,3].

² A good nuclear form factor can be found in Ref. [4]. The spatial charge distribution is parameterized by the Fermi distribution $\rho(\mathbf{r}) = \rho_0/(1 + e^{(r-c)/a_0})$, where the radius at which the density is $\rho_0/2$ is $c = (1.18A^{1/3} - 0.48)$ fm and the edge thickness parameter is $a_0 = 0.57$ fm [5]. The form factor that is valid for nuclei with a well-developed core (i.e., with atomic masses above 20) is obtained by the Fourier transform in the limit $c \gg a_0$,

$$G_E(q) = \left[\frac{\pi a_0}{c} \frac{\sin(qc) \cosh(\pi a_0 q)}{\sinh^2(\pi a_0 q)} - \frac{\cos(qc)}{\sinh(\pi a_0 q)} \right] \frac{4\pi^2 \rho_0 a_0 c}{q},$$

$$\rho_0 = \frac{3}{4\pi c^3} \frac{1}{1 + (a_0 \pi/c)^2}.$$

Note that $G_E(0) = 1$.

$$\frac{d\sigma_{EDM}}{dE_R} = \frac{1}{4\pi} d_\chi^2 Z^2 e^2 \frac{(S + 1)}{3S} \frac{1}{v_r^2} \frac{1}{E_R} |G_E(\mathbf{q}^2)|^2. \quad (2)$$

The $1/(v_r^2 E_R)$ dependence is characteristic of the EDM of the DM particle.³

To have an EDM, the DM particle cannot be self-conjugate. Consequently, for $S = \frac{1}{2}$, the particle has to be Dirac. Note that the spin factor $\frac{S+1}{3S}$ becomes 1 for $S = \frac{1}{2}$ in our numerical illustrations. Our result also applies to the anti-dark matter particle under the assumption that CPT is conserved.

3. Magnetic dipole moment of dark matter

In the static limit, the DM magnetic moment can only couple to the nuclear magnetic moment via the induced magnetic field. The non-relativistic effective Hamiltonian of a magnetic moment of a particle with spin \mathbf{S} subject to a magnetic field \mathbf{B} is, in our convention

$$H_{\text{eff}} = -\mu \mathbf{B} \cdot \mathbf{S}/S,$$

which agrees with the standard form for a spin $\frac{1}{2}$ particle, i.e., $-\mu \mathbf{B} \cdot \boldsymbol{\sigma}$, where μ is dimensionful. Since $\mathbf{B} = \nabla \times \mathbf{A}$, we identify the curl $\nabla \times$ with the momentum transfer $\mathbf{q} \times$. The direct scattering off the nucleus of spin I via the interaction between the nuclear magnetic moments $\mu_{Z,A}$ and the magnetic moment μ_χ of the DM particle is described by

$$\mathcal{M} = \mathbf{S} \times \mathbf{q} \cdot \left(\frac{\mu_\chi}{S} \frac{1}{q^2} \frac{\mu_{Z,A}}{I} \right) \mathbf{I} \times \mathbf{q}.$$

³ The differential reaction rate (per unit detector mass) is

$$\frac{dR}{dE_R} = \frac{\rho_0}{m_\chi} \frac{1}{m_A} \int_{v_{\min}}^{\infty} v_r f_1(v_r) \frac{d\sigma}{dE_R} dv_r,$$

where the local DM density $\rho_0 = 0.3$ GeV/cm³ and $v_{\min} = \sqrt{\frac{m_A E_R}{2m_\chi^2}}$. dR/dE_R includes contributions from both χ and its conjugate $\bar{\chi}$ for they have the same cross sections.

In the non-relativistic limit, the differential cross section can be Maclaurin expanded in powers of v_r . The two most important contributions are

$$d\sigma \sim \frac{1}{v_r^2} d\{\sigma_{-}\} + d\{\sigma_{+}\},$$

with v_r independent coefficients denoted by brackets. (For example, in Eq. (1), $d\{\sigma_{-}\}$ is the coefficient of v_r^{-2} , and $d\{\sigma_{+}\} = 0$.) Usually, the first term is the relevant one (as in the EDM, CFF, or SI cases). However, in certain cases like MDM, the second term may compete due to the $1/E_R$ enhancement from the low energy virtual photon propagator. On integrating, we find

$$\frac{dR}{dE_R} = \frac{\rho_0}{m_\chi} \frac{1}{m_A} \left[\frac{d\{\sigma_{-}\}}{dE_R} \frac{1}{v_0} I_{-} + \frac{d\{\sigma_{+}\}}{dE_R} v_0 I_{+} \right],$$

where the dimensionless integrals are defined by

$$\frac{I_{-}}{N} = \frac{v_0}{2v_E} \left[\text{erf}\left(\frac{v_u}{v_0}\right) - \text{erf}\left(\frac{v_d}{v_0}\right) - \frac{2}{\sqrt{\pi}} \left(\frac{v_u}{v_0} - \frac{v_d}{v_0} \right) e^{-v_{\text{esc}}^2/v_0^2} \right],$$

and

$$\begin{aligned} \frac{I_{+}}{N} = & \left(\frac{v_d}{2v_E \sqrt{\pi}} + \frac{1}{\sqrt{\pi}} \right) e^{-v_d^2/v_0^2} - \left(\frac{v_u}{2v_E \sqrt{\pi}} - \frac{1}{\sqrt{\pi}} \right) e^{-v_u^2/v_0^2} \\ & + \frac{v_0}{4v_E} \left(1 + \frac{2v_E^2}{v_0^2} \right) \left(\text{erf}\left(\frac{v_u}{v_0}\right) - \text{erf}\left(\frac{v_d}{v_0}\right) \right) \\ & - \frac{1}{\sqrt{\pi}} \left[2 + \frac{1}{3v_E v_0^2} ((v_{\min} + v_{\text{esc}} - v_d)^3 - (v_{\min} + v_{\text{esc}} - v_u)^3) \right] e^{-v_{\text{esc}}^2/v_0^2}, \end{aligned}$$

with the shorthand $v_u = \min(v_{\min} + v_E, v_{\text{esc}})$, $v_d = \min(v_{\min} - v_E, v_{\text{esc}})$. Note that $I_{-} = 0$ for $v_{\min} > v_{\text{esc}} + v_E$.

The curl substitution has been applied to the DM vertex and the nuclear vertex which are linked by the virtual photon exchange factor $1/\mathbf{q}^2$. The spin-averaged differential cross section is

$$d\sigma_{MDM}(\chi N) = \frac{2}{\pi} \mu_\chi^2 \mu_{Z,A}^2 \frac{S+1}{3S} \frac{I+1}{3I} \frac{d\mathbf{q}^2}{4v_r^2} |G_M(\mathbf{q}^2)|^2. \quad (3)$$

The magnetic nuclear form factor G_M has been included. The above purely magnetic description ignores an important nuclear charge Z^2 effect which is suppressed by v_r^2 but enhanced by $1/E_R$. Both the magnetic and electric effects are comparable at direct search experiments with low recoil energy thresholds.

To account for the Z^2 effect, we need to treat the convection current of the nucleus $Z(p_{Z,A}^\mu + p_{Z,A}'^\mu)$ (where $p_{Z,A}^\mu$ and $p_{Z,A}'^\mu$ are the incoming and outgoing momenta, respectively) with a Dirac trace calculation. Then we include the above contribution from the nuclear magnetic moment associated with its spin I . The leading contributions for low recoil energy and low relative velocity give

$$\frac{d\sigma_{MDM}}{dE_R} = \frac{e^2 \mu_\chi^2}{4\pi E_R} \frac{S+1}{3S} \left[Z^2 \left(1 - \frac{E_R}{2m_A v_r^2} - \frac{E_R}{m_\chi v_r^2} \right) |G_E|^2 + \frac{I+1}{3I} \left(\frac{\mu_{Z,A}}{2m_p} \right)^2 \frac{m_A E_R}{m_p^2 v_r^2} |G_M|^2 \right]. \quad (4)$$

The two nuclear form factors G_E and G_M are normalized so that $G_E(0) = 1$ and $G_M(0) = 1$; the charge Z and the moment $\mu_{Z,A}$ have been factored out. In our numerical analysis we make the simplifying assumption that the two nuclear form factors G_E and G_M are approximately equal, although they could be slightly different.

Several studies only include the nuclear spin and ignore the effect of the nuclear charge, e.g., Ref. [6]. Others inappropriately scale the result for a Dirac point charge by Z^2 [7,8]. Our result reduces to that of Ref. [8] in the limit that a nucleus becomes a Dirac point charge, $Z \rightarrow 1$, $\mu_{Z,A}/(2m_p) \rightarrow 1$, $m_A \rightarrow m_p$, and $I \rightarrow 1/2$, and has subsequently been reproduced in an erratum to Ref. [9]. It is worth pointing out that a proton with a significant anomalous magnetic moment is not faithfully represented by a Dirac point charge. Note that the A^2 factor in the result of Ref. [10] must be replaced by $(m_A/m_p)^2$ to agree with our expression, and for quantitative accuracy.

4. Electric charge form factor of dark matter

A neutral non-self-conjugate dark matter particle can couple directly to the photon via its charge form factor (CFF) $G_\chi(\mathbf{q}^2)$; charge neutrality only implies $G_\chi(0) = 0$. At low momentum transfer, it is conveniently parameterized by a cutoff Λ_{CFF} :

$$G_\chi(\mathbf{q}^2) = \mathbf{q}^2 / \Lambda_{CFF}^2.$$

The amplitude for DM–nucleus scattering via the form factor is given by

$$\mathcal{M} = G_\chi(\mathbf{q}^2) (e^2 / \mathbf{q}^2) Z G_E(\mathbf{q}^2),$$

which is clearly spin-independent, so that the differential cross section is

$$d\sigma_{CFF}(\chi N) = \frac{e^4 |Z G_E(\mathbf{q}^2)|^2 d\mathbf{q}^2}{\pi \Lambda_{CFF}^4 4v_r^2}. \quad (5)$$

Employing the cutoff Λ_{CFF} translates into a useful cross section for DM–proton scattering:

$$\begin{aligned} \sigma_{CFF}^{(p)} &= \frac{1}{\pi} \frac{m_p^2 m_\chi^2}{(m_\chi + m_p)^2} \left(\frac{e^2}{\Lambda_{CFF}^2} \right)^2 \\ &\simeq \left(\frac{1 \text{ TeV}}{\Lambda_{CFF}} \right)^4 \frac{m_\chi^2}{(m_p + m_\chi)^2} \times 0.92 \times 10^{-42} \text{ cm}^2, \end{aligned}$$

which is relevant to the DM capture rate in the Sun. The proton form factor is essentially flat and ignored during the integration.

In comparison, the SI scattering amplitude,

$$\mathcal{M}_{SI} = 2[f_p Z + f_n(A - Z)] G_E(\mathbf{q}^2)$$

(where we have used the electric form factor to approximate the nuclear size effect), yields the differential DM–nucleus cross section,

$$\frac{d\sigma_{SI}^{(Z,A)}}{dE_R} = \frac{4}{\pi} [f_p Z + f_n(A - Z)]^2 |G_E(\mathbf{q}^2)|^2 \frac{m_A}{2v_r^2},$$

and the DM–proton SI cross section,

$$\sigma_{SI}^{(p)} = \left(\frac{Z}{A} \right)^2 \sigma_{CFF}^{(p)} = \frac{4}{\pi} \frac{m_p^2 m_\chi^2}{(m_\chi + m_p)^2} f_p^2.$$

We therefore have the correspondence,

$$\frac{e^2}{\Lambda_{CFF}^2} Z \longleftrightarrow 2[f_p Z + f_n(A - Z)].$$

If we assume $f_p = f_n = \Lambda_{SI}^{-2}$ for simplicity, we can further simply to the correspondence,

$$\frac{1}{\Lambda_{SI}^2} \longleftrightarrow \frac{1}{2} \left(\frac{Z}{A} \right) \frac{e^2}{\Lambda_{CFF}^2}.$$

Since $2Z \approx A$ for most nuclei, the correspondence becomes

$$\Lambda_{SI} \leftrightarrow \frac{2}{e} \Lambda_{CFF} \approx 6.6 \Lambda_{CFF}.$$

5. Analysis

For the MDM of DM, we define the dimensionless gyromagnetic ratio or g-factor g_χ by

$$g_\chi S = \frac{\mu_\chi}{\frac{e}{2m_\chi}}.$$

It is useful to compare d_χ and μ_χ in terms of the effective cutoff scales Λ_{EDM} and Λ_{MDM} defined by

$$d_\chi \equiv \frac{e}{\Lambda_{EDM}} \quad \text{and} \quad \mu_\chi = g_\chi S \frac{e}{2m_\chi} \equiv \frac{e}{\Lambda_{MDM}}.$$

Then,

$$\frac{\Lambda_{EDM}}{1 \text{ TeV}} = 19733 \times \frac{10^{-21} e \text{ cm}}{d_\chi} \quad \text{and} \quad \frac{\Lambda_{MDM}}{1 \text{ TeV}} = \frac{2}{g_\chi S} \frac{m_\chi}{1 \text{ TeV}}.$$

(Note that the cutoff scales are arbitrarily defined quantities, related to compositeness or short distance physics. They are defined in order to facilitate comparison and are not to be interpreted as new physics scales.) Direct DM search experiments are currently sensitive to $d_\chi \sim 10^{-21} e \text{ cm}$ which translates into a sensitivity to Λ_{EDM} of almost 20 PeV. On the other hand, experiments are sensitive to $g_\chi S \sim 0.001$ or Λ_{MDM} of order 10 TeV for $m_\chi \lesssim 10 \text{ GeV}$. The difference arises because the MDM contribution to direct searches is more non-relativistically suppressed. Due to the higher dimensionality of the DM charge form factor, the corresponding scale Λ_{CFF} can be probed to about a few 100 GeV.

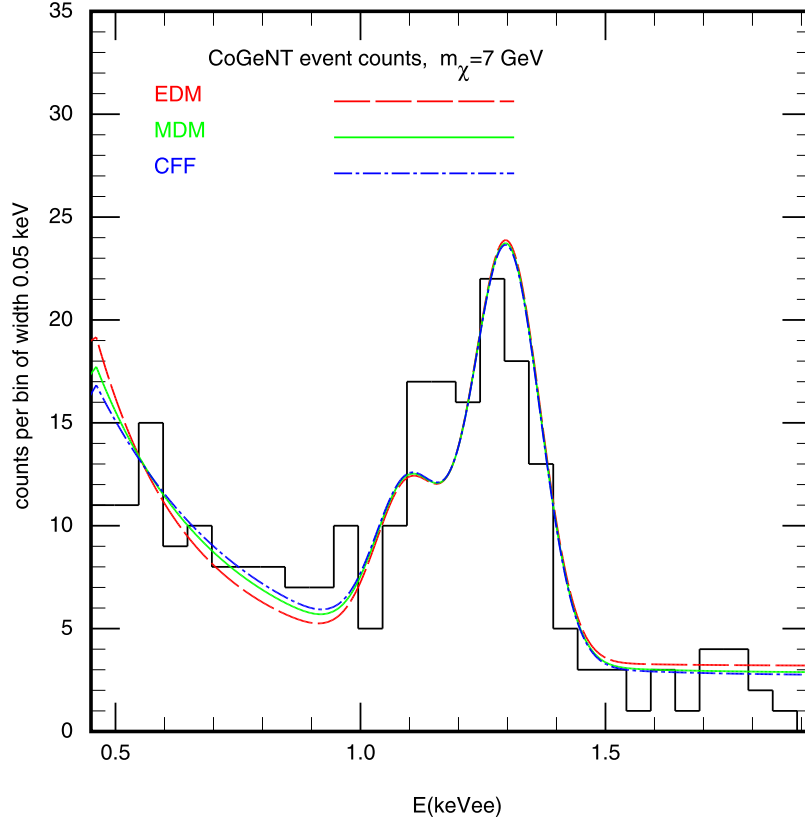


Fig. 1. A DM particle with $m_\chi = 7$ GeV and an EDM, MDM or CFF reproduces CoGeNT data from a 56-day run with 0.33 kg of germanium. Note that the shape of the CFF curve is identical to that for spin-independent scattering.

We now consider the consequences of these electromagnetic properties of DM for direct searches.⁴ Since the DM velocity cannot exceed v_{esc} , which we take to be 600 km/s, a DM particle lighter than 7.2 GeV cannot give a nuclear recoil energy above 10 keV, which was the threshold cut adopted by the CDMS-II Collaboration [12]. Although CDMS-II has accumulated more kg·days of data than CoGeNT [13], the lower threshold energy of CoGeNT permits sensitivity to masses as low as 3 GeV. Solely for the purpose of illustration, we focus on the CoGeNT anomaly.

In Fig. 1, we show that a 7 GeV DM particle with an EDM of $d_\chi = 10^{-20} e \text{ cm}$ (equivalently $\Delta_{\text{EDM}} = 1.97 \text{ PeV}$), or an MDM with $g_\chi S = 0.00454$ (equivalently $\Delta_{\text{MDM}} = 3.09 \text{ TeV}$), or a CFF with $\Lambda_{\text{CFF}} = 187 \text{ GeV}$ (corresponding to $\sigma_{\text{CFF}}^{(p)} = 5.8 \times 10^{-40} \text{ cm}^2$ or $\sigma_{\text{SI}}^{(p)} = 1.1 \times 10^{-40} \text{ cm}^2$) easily reproduces the CoGeNT event excess below 2 keVee; we employed an energy-dependent quenching factor, $E(\text{keVee}) = 0.19935 E_R(\text{keV})^{1.1204}$, which converts the total nuclear recoil energy E_R to the energy detected by the experiment (in the form of ionization, scintillation or heat) with units of equivalent electron energy (keVee). The corresponding χ^2 values

for the 3-parameter fit to 30 data points between 0.45 keVee and 1.9 keVee are $\chi_{\text{EDM}}^2 = 26$, $\chi_{\text{MDM}}^2 = 22$ and $\chi_{\text{CFF}}^2 = 20$, where [14]

$$\chi^2 = \sum_{i \text{ with } N_i^{\text{exp}} \neq 0} 2 \left(N_i^{\text{th}} - N_i^{\text{exp}} + N_i^{\text{exp}} \ln \frac{N_i^{\text{exp}}}{N_i^{\text{th}}} \right) + \sum_{i \text{ with } N_i^{\text{exp}} = 0} 2 N_i^{\text{th}},$$

and the N_i^{th} include a background contribution that is modeled as a linear combination of a constant term and a sum of two weighted Gaussian distributions that describe the peaks from the decay of ^{65}Zn and ^{68}Ge via L-shell electron capture [13]. Two of the fit parameters fix the background and the third parameter normalizes the signal. In all cases, the constant background is about 3 events/bin which explains the data between 1.5 keVee and 3.2 keVee satisfactorily.

Since in all cases the DM–nucleus scattering is dominantly SI, the most stringent constraints in this low m_χ range are obtained from the XENON10 experiment due its low energy threshold [15] (and perhaps CDMS-II silicon detector data [16] which may have an underestimated energy calibration uncertainty). We assert that the DM candidates of Fig. 1 are consistent with the XENON10 data based on the following: (1) The shape of the CFF recoil energy distribution is identical to that for SI scattering, and depending on analysis details, SI scattering of a 7 GeV DM particle with $\sigma_{\text{SI}}^{(p)} \sim 10^{-40} \text{ cm}^2$ is either compatible with [17] or marginally excluded by [18] XENON10 data, (2) the distributions of Fig. 1 are almost identical, and (3) we checked that for $m_\chi = 7$ GeV, the difference in the recoil energy distributions for CFF scattering on Ge and Xe is larger than for scattering via an EDM or MDM. Taking

⁴ The relevant nuclear parameters for the CoGeNT, CDMS and XENON experiments are [11],

$$^{73}\text{Ge}: \quad I = \frac{9}{2}, \quad \mu_{Z,A} = -0.8795 \frac{e}{2m_p}, \quad f = 7.73\%,$$

$$^{129}\text{Xe}: \quad I = \frac{1}{2}, \quad \mu_{Z,A} = -0.778 \frac{e}{2m_p}, \quad f = 26.44\%,$$

$$^{131}\text{Xe}: \quad I = \frac{3}{2}, \quad \mu_{Z,A} = 0.692 \frac{e}{2m_p}, \quad f = 21.18\%,$$

where f is the natural abundance of the isotope.

these facts together, we infer that the DM candidates of Fig. 1 are not in conflict with XENON10 data.

Acknowledgements

We thank J. Collar for providing us with a wee note on CoGeNT data. This work was supported by DoE Grants Nos. DE-FG02-84ER40173, DE-FG02-95ER40896 and DE-FG02-04ER41308, by NSF Grant No. PHY-0544278, and by the Wisconsin Alumni Research Foundation. D.M. thanks the Aspen Center for Physics for its hospitality.

References

- [1] G. Jungman, M. Kamionkowski, K. Griest, Phys. Rep. 267 (1996) 195, arXiv: hep-ph/9506380.
- [2] M.J. Reid, et al., Astrophys. J. 700 (2009) 137, arXiv:0902.3913 [astro-ph.GA].
- [3] M. Drees, C.L. Shan, JCAP 0706 (2007) 011, arXiv:astro-ph/0703651.
- [4] I.Zh. Petkov, et al., Yad. Fiz. 4 (1966) 57, Sov. J. Nucl. Phys. 4 (1967) 41.
- [5] M.A. Preston, R.K. Bhaduri, Structure of the Nucleus, Addison-Wesley Co., Inc., 1975, pp. 87, 88, 100.
- [6] M. Pospelov, T. ter Veldhuis, Phys. Lett. B 480 (2000) 181, arXiv:hep-ph/0003010;
- See also J.H. Heo, arXiv:0902.2643 [hep-ph].
- [7] K. Sigurdson, M. Doran, A. Kurylov, R.R. Caldwell, M. Kamionkowski, Phys. Rev. D 70 (2004) 083501, arXiv:astro-ph/0406355;
- K. Sigurdson, M. Doran, A. Kurylov, R.R. Caldwell, M. Kamionkowski, Phys. Rev. D 73 (2006) 089903.
- [8] E. Masso, S. Mohanty, S. Rao, Phys. Rev. D 80 (2009) 036009, arXiv:0906.1979 [hep-ph].
- [9] W.S. Cho, J.H. Huh, I.W. Kim, J.E. Kim, B. Kyae, Phys. Lett. B 687 (2010) 6, arXiv:1001.0579 [hep-ph].
- [10] J. Bagnasco, M. Dine, S.D. Thomas, Phys. Lett. B 320 (1994) 99, arXiv:hep-ph/9310290.
- [11] R. Leighton, Principles of Modern Physics, McGraw-Hill Book Co., 1959. For recent tabulations with natural isotopic abundances f see <http://www.webelements.com/germanium/isotopes.html>, <http://www.webelements.com/xenon/isotopes.html>.
- [12] Z. Ahmed, et al., CDMS-II Collaboration, Science 327 (2010) 1619, arXiv:0912.3592 [astro-ph.CO].
- [13] C.E. Aalseth, et al., CoGeNT Collaboration, arXiv:1002.4703 [astro-ph.CO].
- [14] C. Amsler, et al., Particle Data Group, Phys. Lett. B 667 (2008) 1.
- [15] J. Angle, et al., XENON Collaboration, Phys. Rev. Lett. 100 (2008) 021303, arXiv:0706.0039 [astro-ph];
- J. Angle, et al., Phys. Rev. D 80 (2009) 115005, arXiv:0910.3698 [astro-ph.CO].
- [16] J.P. Filippini, PhD thesis, University of California, Berkeley, 2008;
- J. Filippini, CDMS Collaboration, Nuovo Cimento C 32 (2009) 45.
- [17] D. Hooper, J.I. Collar, J. Hall, D. McKinsey, arXiv:1007.1005 [hep-ph].
- [18] P. Sorensen, arXiv:1007.3549 [astro-ph.IM].